Since January 2020 Elsevier has created a COVID-19 resource centre with free information in English and Mandarin on the novel coronavirus COVID-19. The COVID-19 resource centre is hosted on Elsevier Connect, the company's public news and information website.

Clinical Imaging 79 (2021) 265–272

Contents lists available at ScienceDirect

Clinical Imaging

journal homepage: www.elsevier.com/locate/clinimag

Pediatric Radiology

Correlation of laboratory parameters and Chest CT findings in young adults with COVID-19 and comparison of imaging findings with children☆

Zuhal Bayramoglu [a,*], Eda Cingoz [a], Rana G. Comert [a], Nilufar Gasimli [a], Ozge Kaba [b], Mehpare Sari Yanartas [b], Selda Hancerli Torun [b], Ayper Somer [b], Sukru Mehmet Erturk [a], Atadan Tunaci [a]

[a] Istanbul University, Istanbul Medical Faculty, Radiology Department, Turkey
[b] Istanbul University, Istanbul Medical Faculty, Department of Pediatric Infectious Disease, Turkey

ARTICLE INFO

Keywords:
COVID-19
Computed tomography
Children
Young adults

ABSTRACT

Purpose: We aimed to compare COVID-19 imaging findings of young adults (19–35 years of age) with those of children (0–18 years) and to correlate imaging findings of young adults with their laboratory tests.

Materials and methods: This retrospective study included Real Time-Polymerase Chain Reaction (RT-PCR) confirmed 130 young adults (mean age: 28.39 ± 4.77; 65 male, 65 female) and 36 children (mean age: 12.41 ± 4.51; 17 male, 19 female), between March and June 2020. COVID-19 related imaging findings on chest CT were examined in young adults and compared with children by the Mann-Whitney U, and Chi-square or Fisher's exact test. Laboratory examinations of young adults were assessed in terms of correlation with radiological findings by the Spearman's correlation analysis.

Results: Bilateral multiple distributions ($p = 0.014$), subpleural involvement, and pleural thickening ($p = 0.004$), GGOs with internal consolidations were more frequent in adults ($p = 0.009$). Infiltrations were significantly larger than 20 mm in young adults ($p = 0.011$). The rates of feeding vessel sign, vascular enlargement, and halo sign were significantly higher in young adults ($p < 0.003$). Highly significant positive correlations were found between radiological and biochemical parameters.

Conclusion: Distribution, size, and pattern of COVID-19 related imaging findings differed in children and young adults. Radiological findings were correlated with biochemical parameters but not with blood count results of young adults.

1. Introduction

2019-nCoV is an enveloped and single-stranded RNA virus which is a member of the beta-CoVs family and has a zoonotic origin.[1] Although bats were initially identified as natural hosts, currently the primary source is infected people. The virus infects the cells through the angiotensin-converting enzyme-2 protein found in the lung, intestines, heart, and kidney.[2] Infected people may be asymptomatic or develop mild to severe clinical findings, commonly as fever and cough often associated with lymphopenia in blood count. Overactivation of T lymphocytes owing to systemic viral sepsis may result in cytokines storm and acute respiratory distress syndrome or even death.[2] Pathological findings in the lungs include bilateral diffuse alveolar damage, hyaline membrane formation, lymphocyte-weighted mononuclear cell infiltration in the interstitium, and changes consistent with viral cytopathy similar to Severe Acute Respiratory Syndrome and the Middle East Respiratory Syndrome.[3] Thromboses of small or middle-sized pulmonary arteries due to local prothrombotic mechanisms associated with dyspnea, hypoxia, and radiological findings were frequently depicted in elderly patients.[4] Age was depicted as an independent risk factor for disease severity[5] and also COVID-19 related deaths with a male predilection.[6] Disease severity in COVID-19 is associated with blood cell alterations, CRP levels, hemostatic laboratory disorders, and inflammatory markers. A minimal laboratory testing owing to the

☆ The authors declare that they have all participated in the design, execution, and analysis of the paper, and they have approved the final version. Additionally, there are no conflicts of interest in connection with this paper, and the material described is not under publication or consideration for publication elsewhere. No financial support was taken during the paper was preparing.

* Corresponding author at: Department of Radiology, Istanbul Medical Faculty, Istanbul University, Fatih, Millet Street, 34390 Istanbul, Turkey.
E-mail address: incezuhal@yahoo.com (Z. Bayramoglu).

https://doi.org/10.1016/j.clinimag.2021.06.012
Received 20 March 2021; Received in revised form 2 June 2021; Accepted 3 June 2021
Available online 18 June 2021

prognostic monitorisation was suggested.[7] The relationship of radiological findings with laboratory tests was depicted in a few studies in elderly patients.[8,9] There have been limited data regarding the radiological and laboratory findings of younger patients with COVID-19 diagnosis along with the possible association.

Radiological findings of COVID-19 have been extensively investigated in the middle-aged and older adults as bilaterally and peripherally distributed ground-glass opacities (GGOs), which were either rounded or patchy in shape commonly associated with subpleural involvement.[10] Chest CT manifestations of COVID-19 have been variable in different age groups.[11–14] In a study with the largest pediatric population, normal CT examinations were depicted in 77% of children.[15] Radiological differences of COVID-19 in children compared to adults have been depicted in a few studies with small sample sizes.[11,15–20] Comparisons between younger age groups were limited due to mild clinical courses and relatively higher asymptomatic cases in children. Although clinical and radiological correlations have been extensively investigated, the correlation of radiological findings with laboratory tests has not yet been confirmed.

In this study, we aimed to reveal COVID-19 related imaging findings in young adults, compare the findings with children, and assess the data of young adults for correlation with laboratory changes.

2. Material and methods

2.1. Study protocol and patients

The current retrospective study was performed in a single academic center and included young adults and children diagnosed with COVID-19 with RT-PCR tests between 10 March and 15 October 2020. The local ethics committee approved the study (File number: 2020/1101). Informed consent was waived because of the retrospective design. RT-PCR tests were evaluated in two laboratories under the supervision of the Ministry of Health. One hundred and thirty young adults aged 19–35 years (65 male, mean age: 28.70 ± 4.63 years; 65 female, mean age: 28.09 ± 4.96 years) and 36 children aged 0–18 years (17 male, mean age: 11.47 ± 4.18 years; 19 female, mean age: 13.26 ± 4.74 years) were included. None of the children had a chronic cardiac, pulmonary, or hepatic disease that may lead to lymphadenopathy, pleural effusion, or pulmonary interlobular interstitial thickening which may mimic COVID-19 related findings. Among the young adults, four patients had chronic kidney failure, four patients had hypothyroidism, two patients had multinodular goiter, two patients had hypertension, two patients had a history of kidney transplantation, one patient had asthma, one patient had metabolic syndrome, one patient was operated for rectum cancer and one patient was operated for thyroid carcinoma. But none of the patients had any finding of a decompensated organ failure at the time of the radiological examination. We retrieved initial chest CT examinations of 36 children and 130 young adults, one for each patient. We included a proportional number of symptomatic children and young adults with the general hospital admission. The number of young adult patients was not reduced in order not to weaken the laboratory correlation of this group. Other causes of ground-glass opacity could not be ruled out via viral swab paned owing to the pandemic circumstances.

2.2. Clinical laboratory tests

Laboratory test evaluations of young adults were carried out in the same local laboratory on the day of CT examination. White blood cell (WBC), neutrophil, lymphocyte, and platelet levels were collected from the complete blood count database (n:92). We recorded C-reactive protein (CRP, n:91), lactic acid dehydrogenase (LDH, n:85), fibrinogen (n:83), D-dimer (n:89), procalcitonin (n:79), and troponin (n:89) levels. Ferritin levels were depicted in 85 patients, with the references ranged from 30–400 ng/mL to 13–150 ng/mL for the males and females, respectively.

2.3. Chest CT examination

Chest CT examinations of young adults and children with RT-PCR confirmed COVID-19 diagnosis was performed using a 64 detector CT scanner (Aquillon 64, Toshiba Medical Systems, Tochigi, Japan) without using contrast agents (For adult patients, tube voltage, 100–120 kV; tube current time product, 50–150 mAs; reconstruction interval, 1-5 mm; pitch, 0.65–1.4; slice thickness, 5 mm). The exposure dose was adjusted based on the patient's age and weight for the children, varying between 55kVp, 5 mAs, and 100 kVp, 100 mAs. Cooperative patients were ordered to hold their breath. Few studies especially for the patients under three years old had motion artifacts that did not allow the assessment. CT scans with motion and respiratory artifacts that cause diagnostic dilemma due to poor image quality are excluded. All chest CT images were reviewed in terms of COVID-19 related imaging findings with the consensus of a pediatric radiologist (with more than four years of pediatric radiology and nine years of radiology experience) and a radiologist having more than three years of chest radiology experience who were blinded to the symptoms and laboratory tests paying attention to suggestions of Fleischner Society.[21] Pulmonary vascular changes and perivascular distribution (Figs. 1a, 1b, 1c), nodular shaped GGOs and consolidations (Figs. 2a, 2b, 2c, 2d), and COVID-19 involvement in children (Figs. 3a, 3b, 3c, 3d, 3e, 3f) were depicted. The lesions compatible with chronic sequela or not associated with COVID-19 were not included.

Distributions of infiltrations (unilateral or bilateral; central or peripheral; upper, middle or lower lobe; anterior, middle, or posterior zone), and the total number of involved lobes in each case were recorded. An involvement score for each lobe were given based on the infiltration ratio as 1–25%, 26–50%, 51–75% and 76–100% involvement corresponding to 1,2,3,4 score(s), respectively. The total CT involvement score was depicted as the sum of lobes' scores for each patient.[11] We evaluated a pulmonary involvement score based on the segmental involvement to reveal the differences owing to the smaller-sized but multiple opacities. The pulmonary involvement score for each patient was calculated as the sum of the scores of each lung segment (0 for an intact segment, 1 for <50% involvement, and 2 for >50% involvement). We determined the size category of the infiltrates (0-20 mm, 20–40 mm, and >40 mm) based on the size of the largest infiltration.

The involvement pattern as focal or peribronchial along with the subpleural extension, as well as the presence of pleural thickening was

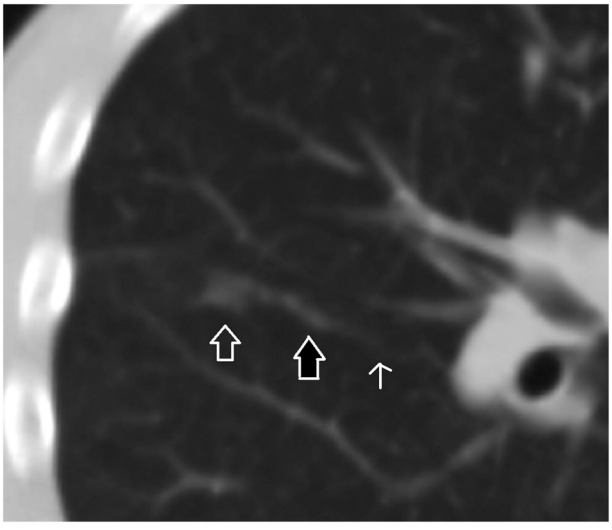

Fig. 1a. A 16-year-old male patient. A focal ground-glass opacity in the anterolateral segment of the right lower lobe located at the tip of the pulmonary artery branch. There is a dense and dilated vessel (closed arrow) compared to the proximal segment (open arrow) just before the infiltrate.

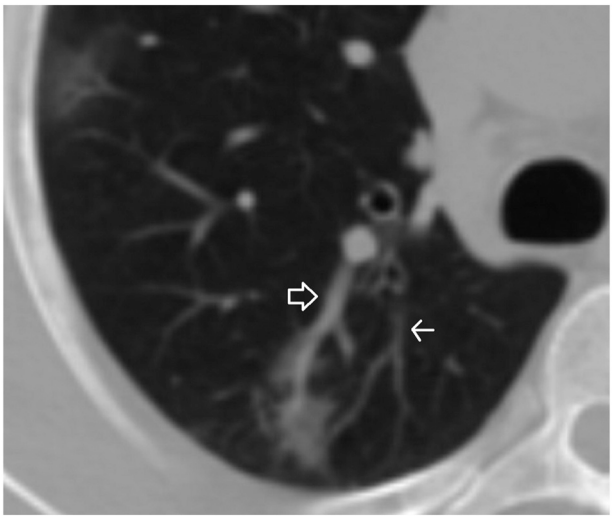

Fig. 1b. A 35-year-old male patient. A ground-glass opacity and associated dilated pulmonary artery (closed arrow) compared to the closest pulmonary artery branch (open arrow).

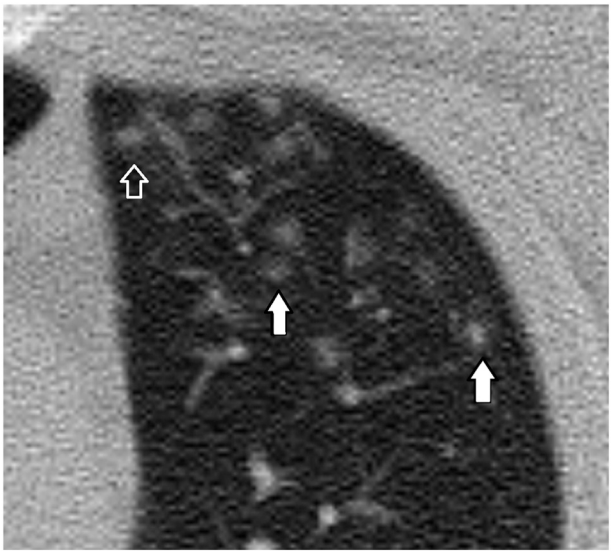

Fig. 1c. A 21-year-old male patient. Nodules at the tips of the pulmonary artery branches (closed arrow) mimicking tree in bud sign are seen. There are multiple nodular ground-glass opacities with an internal dot-like density (White arrow) corresponding to the dense vessels at the center of the infiltrates.

noted. Subpleural involvement was defined as the infiltration adjacent to the pleura. Infiltration density was categorized as pure GGO, GGO with internal consolidation (<50%, >50%), and consolidation. Bronchovascular interstitial thickening and air bronchograms were checked. Imaging findings associated with COVID-19 as the halo sign, vascular enlargement sign, blood vessel penetration sign, vacuole sign, crazy paving pattern, atoll sign (reversed halo), and white lung were investigated. The presence of discrete pulmonary nodules, lymphadenopathy, pleural effusion, atelectasis, and bronchus deformation was evaluated.

2.4. Statistical analysis

We assessed the statistical analysis using the Statistical Package for the Social Sciences (SPSS) (version 21, IBM Corp.). Distribution of the data was tested by the Kolmogorov-Smirnov test with paying attention to skewness and kurtosis. Categorical variables were expressed as a

Fig. 2a. A 20-year-old female patient. Bilateral, nodular shaped, and perivascular distributed GGOs with central consolidations.

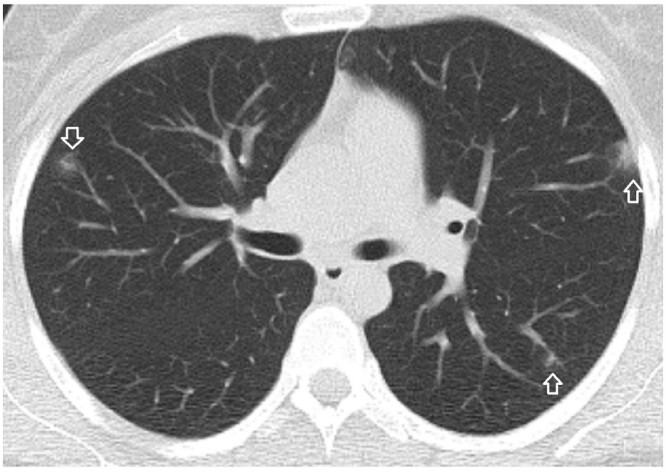

Fig. 2b. A 26-year-old female patient. Bilateral, multiple, peripherally, and perivascular distributed GGOs with subpleural involvement and dense vessels in the centers.

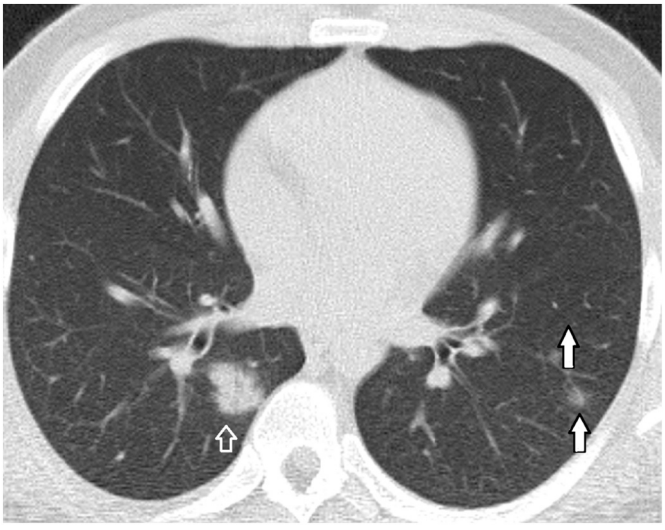

Fig. 2c. A 21-year-old male patient. Bilateral, multiple, peripherally distributed infiltrations both as perivascular GGOs or nodular shaped consolidation.

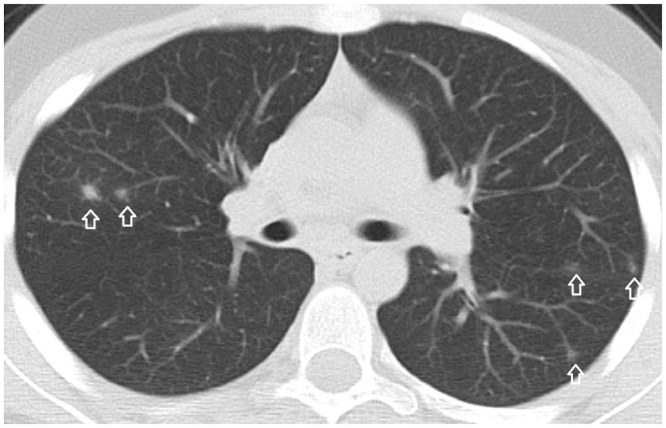

Fig. 2d. A 13-year-old male patient. Bilateral, multiple, peripherally, and perivascular distributed GGOs with dense vessels in the centers.

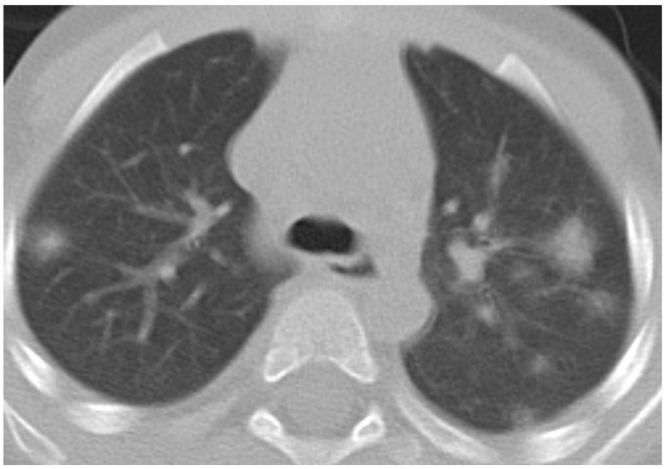

Fig. 3a. 3-year-old male patient. Bilateral peripherally distributed nodular-shaped GGOs and consolidations with halo sign.

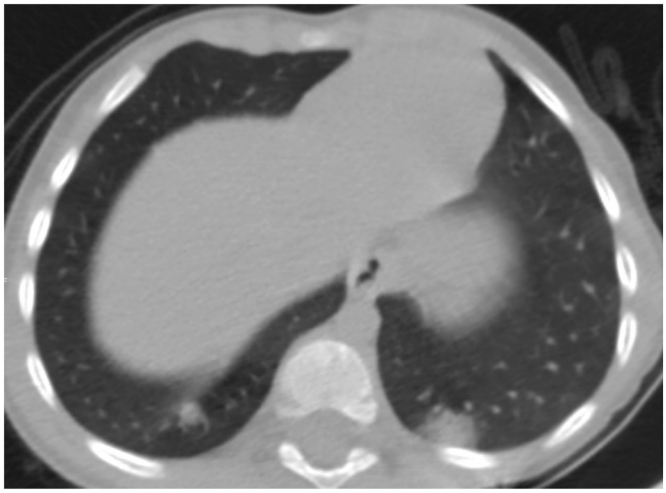

Fig. 3b. 3-year-old male patient. A peripheral nodular-shaped consolidation in the right lung posterobasal segment and a subpleural segmental consolidations with halo sign in the left lung posterobasal segment.

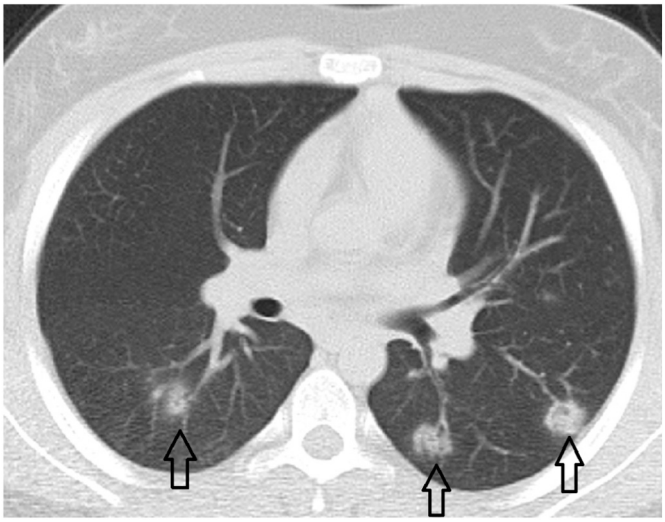

Fig. 3c. 13-year-old female patient. Bilateral peripheral and perivascular distributed nodular shaped consolidations associated with halo sign.

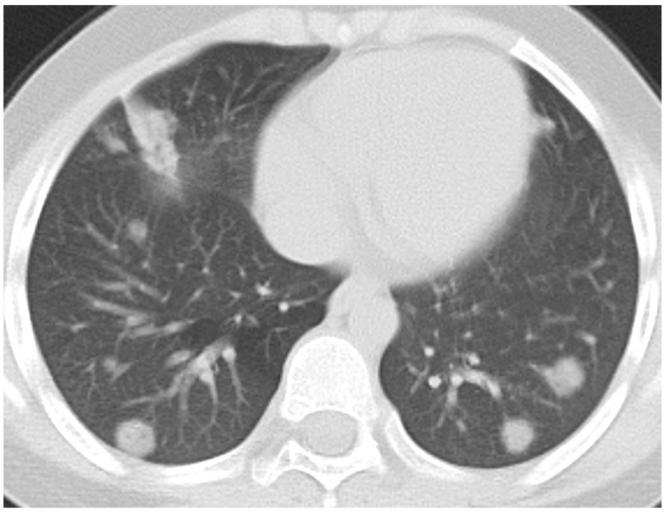

Fig. 3d. 9-year-old male patient. Bilateral peripheral/subpleural nodular-shaped perivascular consolidations and a segmental patchy consolidation at the right lung middle lobe.

percentage and assessed using the Chi-square or Fisher's exact tests among the children and young adults. Non-parametric data were expressed as median (IQR) and compared with the Mann-Whitney *U* test. The parametric data were expressed as mean ± standard deviation and compared with the *t*-test among children and young adults. Spearman's correlation analysis was performed to assess the association between radiological and laboratory data. A *p*-value of less than 0.05 is considered as statistically significant.

3. Results

The descriptive statistics of age and quantitative radiological parameters in young adults compared to children are given in Table 1. There were no statistically significant differences regarding the medians of the largest infiltration size ($p = 0.079$), the total number of involved lobes ($p = 0.6$), CT involvement score ($p = 0.99$), and pulmonary involvement score ($p = 0.76$) between young adults and children.

Chest CT examination results are given in Tables 2, 3. 52.7% of the 36 children and 53.8% of the young adults have abnormal findings

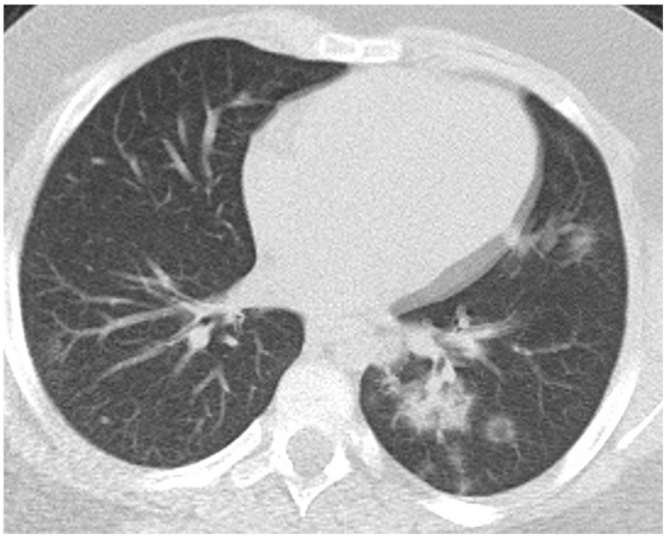

Fig. 3e. 9-year-old male patient. Bilateral peripheral multifocal GGOs and subsegmental patchy consolidation at the lower lobe of the left lung.

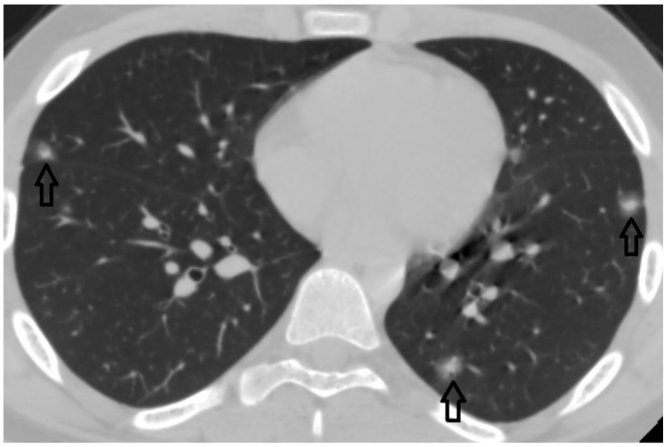

Fig. 3f. 14-year-old male patient. Bilateral multifocal subcentimeter nodular-shaped GGOs with central consolidations.

Table 1
Descriptive statistics comparison of quantitative parameters in children and young adults

Parameter	0–18 years (n:36)		19–35 years (n:130)		p
	Mean ± standard deviation	Median (IQR)	Mean ± standard deviation	Median (IQR)	
Age	12.41 ± 4.51	14 (9.25–16)	28.39 ± 4.77	29 (25–33)	0.001*
Largest lesion size (mm)	17.47 ± 25.91	8 (5–15.5)	28.4 ± 25.99	16 (6–45)	0.079
Total number of involved lobes	2.35 ± 1.53	2 (1–3.5)	2.47 ± 1.53	2 (1–4)	0.6
CT involvement score	2.7 ± 1.75	2 (1–4)	2.7 ± 1.86	2 (1–4)	0.99
Pulmonary involvement score	2.85 ± 2.75	1.5 (1–4.25)	4.89 ± 4.25	2 (1–6)	0.76

P-values by Mann-Whitney *U* test, *p-value by t-test.
IQR: Interquartile range.

related to COVID-19 on chest CT exams. Lower lobes were more frequently affected in both young adults (n:58, 44.6%) and children (n:17, 47.2%) without statistical significance. Bilateral multiple infiltrations were more frequently depicted in adults compared to children ($p = 0.014$). Subpleural involvement ($p = 0.004$) and associated pleural thickening ($p = 0.001$) were more frequently seen in young adults compared to children. Lesions were peripherally distributed in a considerable number of young adults (51.5%) and children (52%) (Figs. 2a, 2b, 2c, 2d, 3f). There was no preponderance in terms of anterior and middle distribution in age groups. Infiltrations were significantly larger than 20 mm in young adults compared to children ($p = 0.011$). Infiltrations were either nodular-shaped or peribronchial distributed in both children and young adults (Figs. 2a, 2c, 3a, 3b, 3c, 3d, 3f) . GGOs with or without consolidation were more frequent in both age groups compared to pure consolidations. GGOs were more frequently associated with internal consolidations in adults compared to children ($p = 0.009$) (Fig. 2c). The rates of feeding vessel sign ($p = 0.001$), vascular enlargement (p = 0.001), and halo sign ($p = 0.003$) were significantly higher in young adults compared to children (Figs. 1b, 1c). Discrete nodules were frequently depicted both in children (n:11; 30.5%) and young adults (n:46, 35.4%). Vacuole sign and air bronchograms were less frequently depicted imaging findings with a slightly higher incidence in young adults . Bronchovascular interstitial thickening and lymphadenopathy were more frequent in children without statistical significance. Pleural effusion was depicted in only a child (2.7%) but not in adults. Atoll sign (n:2,1.5%) and crazy paving pattern (n:4, 3%) were less frequently depicted findings in young adults but not seen in children. Bronchus deformation, white lung, and tree in bud sign were not depicted in both children and young adults.

The descriptive statistics of non-normal distributed laboratory parameters in young adults are given in Table 4. The leukocyte (n:72, 78.3%), neutrophil (n:77, 83.7), lymphocyte (n:69, 75%), platelet (n:84, 91.3), fibrinogen (n:48, 57.8), D-dimer (n:73,83%), CRP (n:50, 54.3%), troponin (n:86, 96.6), LDH (n:68, 80%), ferritin (n:65, 85.6%), and procalcitonin (n:79, 97.5%) levels were normal in considerable number of the young adults. Lymphopenia (n:23, 25%), leukopenia (n:15, 16.3%), neutropenia (n:12, 13%), and thrombocytopenia (n:7, 7.6%) were the most frequent complete blood count alterations, respectively. Elevated CRP (n:41, 45%) and fibrinogen (n:35, 42.2%) levels were more frequently encountered compared to blood count alterations. LDH (n:9, 10.6%) and D-dimer (n:16, 18%) elevations were less frequently depicted biochemical findings. The incidences of elevated troponin (n:3, 3.4%) and procalcitonin (n:2, 2.5%) levels were lower than frequency of blood count alterations.

Correlation analysis results are shown in Table 5. Statistically significant moderate positive correlations were found between radiological and biochemical parameters. Highly significant moderate positive correlations were found between CRP and all quantitative radiological parameters ($p = 0.041$ - <0.001, $r = 0.21$–0.47). LDH levels were significantly correlated with the CT involvement score, pulmonary involvement score, and the total number of involved lobes. Fibrinogen levels were correlated with lesion size, size range category, and also the total number of involved lobes. Ferritin levels were correlated with lesion size and size category. D-dimer levels were correlated with the scores of pulmonary involvement and also the total CT involvement. No significant correlations were depicted among the quantitative radiological parameters with leukocyte, neutrophil, lymphocyte, and platelet counts. Age was positively correlated with pulmonary involvement score ($r = 0.19$, $p = 0.026$) and LDH ($r = 0.25$, $p = 0.019$). A mild negative correlation was found between age and lymphocyte count ($r = -0.24$, $p = 0.018$) but not with radiological findings.

4. Discussion

In the present study, we documented the radiological findings of RT-PCR confirmed COVID-19 in young adults compared to children.

Table 2
COVID-19 related imagings based on distribution and size on chest CT in young adults compared to children. Bold *p*-values depict the significant differences between age groups by Chi-Square test / * Fisher's exact test

Parameter			0–18 years (n:36)	19–35 years (n:130)	p
			Number (Percentage, %)	Number (Percentage, %)	
Abnormal findings			21 (58.3)	70 (53.8)	0.66
Involvement	Unilateral		8 (22.2)	31 (23.8)	Unilateral vs bilateral; 0.9
	Bilateral		9 (25)	37 (28.4)	
	Lower lobe		13 (36.1)	58 (44.6)	0.46
	Total number of involved lobes	1,2	11 (30.5)	42 (32.3)	1,2 vs ≥3 lobes; 0.82
		≥3	6 (16.6)	26 (20)	
Lesion distribution	Single lesion		6 (16.6)	20 (15.3)	0.95
	Unilateral multiple lesions		8 (22.2)	11 (8.4)	**Unilateral vs bilateral multiple lesions; 0.014**
	Bilateral multiple lesions		6 (16.6)	37 (28.4)	
Largest lesion size range	0–20 mm (1)		15(41.6)	36 (27.6)	**1 vs 2,3; 0.011***
	20–40 mm (2)		0	9 (6.9)	
	>40 mm (3)		2 (5.5)	22 (16.9)	
Central-peripheral	Central		3 (8.3)	11 (8.4)	0.95
	Peripheral		19 (52)	67 (51.5)	
Antero-posterior distribution	Posterior		12 (33.3)	58(44.6)	0.077*
	Anterior		7 (19.4)	34(26.1)	0.37
	Middle		10 (27.7)	32(24.6)	0.55

Table 3
COVID-19 related imagings based on distribution and size on chest CT in young adults compared to children. Bold p-values depict the significant results

Parameter		0–18 years (n:36)	19–35 years (n:130)	p
		Number (Percentage, %)	Number (Percentage, %)	
Pleural-subpleural changes	Pleural thickening	3 (8.3)	40 (30.7)	**0.001**
	Pneumonic involvement	9 (25)	51 (39.2)	**0.004**
Infiltration pattern	Nodular	13 (36.1)	38 (29.2)	**0.033**
	Peribronchial	4 (11)	41 (31.5)	
Infiltration density	GGO	7 (19.4)	20 (15.4)	GGO vs consolidation; 0.79
	GGO+ Consolidation (<50%)	2 (5.5)	21 (16.1)	**GGO with consolidation; 0.009**
	GGO+ Consolidation (>50%)	2 (5.5)	8 (6.1)	
	Consolidation	6 (16.6)	23 (17.7)	
Associated findings	Penetrating vessel sign	14 (38.9)	64 (49.2)	**0.001**
	Vascular enlargement	1 (2.7)	37 (28.4)	**0.001**
	Halo sign	7 (19.4)	44 (33.8)	**0.003**
	Vacuole sign	1 (2.7)	7 (5.4)	0.67
	Discrete nodules	11 (30.5)	46 (35.4)	0.5
	Bronchovascular thickening	4 (11.1)	3 (2.3)	0.062
	Air bronchogram	1 (2.7)	10 (7.6)	0.28
	Lymphadenopathy	3 (8.3)	2 (1.5)	0.08*
	Atelectasis	7 (19.4)	9 (7)	**0.02***

Posteriorly and peripherally distributed GGOs with internal consolidations involving commonly less than three lobes were the most common imaging findings in patients younger than 35 years old (Figs. 2a, 2c). Compared to children, multiple lesions were more frequently seen bilateral in adults (Figs. 2a, 2b, 2c). Infiltrates larger than 2 cm, consolidations within GGOs, and peribronchial distribution were more frequent findings in young adults (Fig. 2c). Infiltrates were mostly nodular-shaped in children (Figs. 2d, 3a, 3b, 3c, 3d, 3f). The rates of feeding vessel sign, vascular enlargement, halo sign, and subpleural changes were significantly higher in adults (Figs. 1b, 1c, 2b). Elevated CRP and fibrinogen levels were more common disorders than blood count alterations. Involvement scores and the lesion size were significantly correlated with CRP, LDH, fibrinogen, ferritin, and D-dimer levels. CRP was the most frequently correlated laboratory parameter with the highest degree.

The CT involvement score and the number of total involved lobes in young adults were similar to children in the current study. The mean and median lung segment based pulmonary involvement scores and the largest lesion size was higher in young adults than children without a statistical significance. This may be owing to either higher numbers or larger sizes of lesions. As far as we know, there has been no comparable study based on segmental involvement scores in children and young adults. A recent study revealed a significantly higher number of involved lobes in adults (mean age: 50.34 ± 16 years) than children[11] which may confirm the increased numbers of lesions by age. On the other hand, incidences of larger-sized infiltrations, consolidation associated GGOs, bilaterally distributed multiple lesions in adults compared to children support that children may have milder COVID-19 related findings compared to adults consistent with the literature.[12,13,18] Pleural thickening was more frequent in young adults than children consistent with the literature.[13,15] Similarly, the crazy-paving pattern was relatively lower, and bronchus distortion was not encountered in our cohort than that of middle-aged and elderly patients examined in the literature suggesting milder interstitial changes in younger patients.[22,23] In the current study and relevant literature, the predominantly peripheral distribution in all age groups was revealed due to the microvascular thrombosis and associated pneumonic infiltrations around small-sized vessels.

Nodular-shaped infiltrations are a well-known entity for airway infiltrations due to the development of alveolar communication among preschool children. However, the considerable incidence of nodular-shaped COVID-19-associated pneumonic infiltrations in adults is astounding and not expected for typical bacterial or viral pneumonia. The higher incidence of nodular-shaped infiltrations in children and a considerable number of rounded lesions in adults are compatible with the literature.[15,24] The presence of discrete nodules and multiple

Table 4
Descriptive statistics of the laboratory tests evaluated in young adults (19–35 years of age)

Laboratory tests	Category	Frequency (n (percentage))	Median (IQR)
Leukocyte x10^9/L	Normal	72 (78.3)	6.23 (5.16–7.3)
	Decreased	15 (16.3)	3.5 (3.12–3.65)
	Increased	5 (5.4)	12.79 (11.51–18.84)
Neutrophil x10 9/L	Normal	77 (83.7)	3.82 (2.97–4.76)
	Decreased	12 (13)	2.22 (1.44–2.40)
	Increased	3 (3.3)	8.36 (8.22–8.5)
Lymphocyte x10 9/L	Normal	69 (75)	1.78 (1.4–2.21)
	Decreased	23 (25)	0.84 (0.61–1.08)
Platelets x10 9/L	Normal	84 (91.3)	237 (196–296)
	Decreased	7 (7.6)	140 (109–144.75)
Fibrinogen (mg/dL)	Normal	48 (57.8)	310.5 (278.25–332.25)
	Increased	35 (42.2)	423 (385–462)
D-Dimer (ng/mL)	Normal	73 (82)	300 (270–375)
	Increased	16 (18)	865 (680–1425)
CRP (mg/L)	Normal	50 (55)	1.47 (0.93–2.69)
	Increased	41 (45)	9.33 (7.32–23.18)
Troponin (ng/mL)	Normal	86 (96.6)	3 (3–3)
	Increased	3 (3.4)	30.61 (21−130)
LDH (U/L)	Normal	68 (80)	176 (159–196.5)
	Decreased	8 (9.4)	126.5 (121.75–129.5)
	Increased	9 (10.6)	325 (259.5–354.5)
Ferritin (ng/mL)	Normal	65(85.6)	203 (45–363)
	Decreased	11 (12.9)	9.96 (7.53–18.20)
	Increased	9 (10.58)	562 (286.25–2323.70)
Procalcitonin	Normal	77 (97.5)	0.04 (0.02–0.06)
	Increased	2 (2.5)	1.25 (0.55–1.94)

nodular consolidations with the halo sign may be seen due to different pneumonia agents such as fungal organisms. However, they are not typical for bacterial pneumonia and virus other than SARS-CoV-2. Multiple nodular consolidations associated with the halo and the feeding vessel signs and nodular shaped GGOs with dense internal vessels correspond to SARS-CoV-2 induced microthrombosis, and angiocentric inflammation has not been highlighted in elderly adults but common in younger patients.

Complete blood count testing for detection of lymphopenia, neutrophilia, and thrombocytopenia; fibrinogen, D-dimer, prothrombin time for the depiction of consumption coagulopathy; procalcitonin levels to reveal bacterial coinfection; CRP and ferritin levels for an inflammatory response; LDH for lung or multiple organ injuries; troponin for cardiac injury are recommended as a prognostic laboratory screening panel.[7] It has been shown that the mild or common type COVID-19 associated with the presence of GGO, the involvement of fewer than three lobes, and the halo sign were more frequent under the age of 40 years[23] with increased CRP levels in one of two patients with the highest rate of deterioration among laboratory examinations. Increased CRP values (46%), followed by lymphopenia (43%) and procalcitonin increase (40%) were the most commonly deteriorating laboratory parameters above 40 years of age with the CRP most correlated parameter to pulmonary inflammation index.[9] CRP has been correlated with CT severity score,[8] the number of affected lobes, area, and Hounsfield Unit of the largest lesion.[25] In the present study, we revealed significant correlations of CRP with the radiological parameters regarding the lesion size and distribution, with increased levels in 45% of the young adults that are lower than older adults (84%).[25] Lymphopenia, thrombocytopenia, and neutropenia were less frequently depicted in our cohort than the recent studies covering middle-aged and older adults.[9,23,25] Thrombocytopenia and increased fibrinogen levels were depicted as independent risk factors for disease severity among the patients above 40 years of age[5] but not for death events.[26] We depicted elevated fibrinogen levels as the second most common deteriorated parameter (42%) significantly correlated with lesion size and the number of involved lobes. Based on our knowledge, no comparable data are existent in terms of the correlation of the ferritin and fibrinogen levels with radiological parameters. Elevated procalcitonin was also a predictor of the COVID-19 severity in the elderly population and revealed a moderate correlation with air bronchograms but not with the number of affected lobes or lesion area.[25,27] However, procalcitonin levels were less frequently decreased in young adults (2.5%), and no significant correlations were depicted with radiological parameters. Based on the results of a meta-analysis, LDH levels were found among the more common laboratory findings following increased CRP and lymphopenia.[28] Although LDH levels were less commonly above the normal limit (10.6%) in young adults, it presented the second most significantly correlated parameter with CT involvement score. D-dimer levels have been associated with death events.[26] We depicted significant correlations with D-dimer and pulmonary involvement score followed by CT involvement score but not with lesion size in the current study. However, D-dimer levels were moderately correlated with the area of the maximal lesion in elderly patients.[25] Despite the milder laboratory changes in young adults compared to older adults, laboratory findings were strongly correlated with radiological findings in young adults except for the blood count results.

Our study has some limitations. First, the correlation between laboratory and radiology findings was not assessed in the pediatric group due to the limited data owing to milder clinical courses. Second, clinical parameters such as concomitant drug use in the young adult age group were not investigated due to the retrospective design. However, we think that the minor accompanying conditions will be less common compared to older adults. Third, the time between the patients' contact and the onset of symptoms to the CT examination was not obtained. However, laboratory examination and radiological evaluation were obtained simultaneously. Initial CT examinations of the patients in the first week from the onset of symptoms were evaluated, and sequelae or involutional changes were not included. Finally, other pneumonia factors and causes of microvascular thrombosis could not be ruled out due to the failure of viral respiratory test panels acceptance during the peak period.

In conclusion, COVID-19 related imaging findings revealed some differences among young adults and children. Radiological findings were strongly correlated with biochemical parameters but not blood count results.

Table 5
Spearman's correlation analysis of laboratory tests with radiological findings in young adults (19–35 years of age)

	Fibrinogen		D-dimer		CRP		Ferritin		LDH		Lymphocyte	
	p	r	p	r	p	r	p	r	p	r	p	r
Number of involved lobes	**0.03**	**0.3**	0.08	0.24	**0.003**	**0.4**	0.22	0.17	**0.004**	**0.39**	0.17	−0.18
CT involvement score	0.12	0.35	**0.02**	**0.31**	**0.001**	**0.46**	0.18	0.18	**0.001**	**0.43**	0.13	−0.2
Largest lesion size	**0.036**	**0.3**	0.48	0.09	**0.002**	**0.41**	**0.021**	**0.32**	0.32	0.14	0.54	−0.08
Largest lesion size range	**0.001**	**0.44**	0.35	0.13	**0.001**	**0.47**	**0.047**	**0.27**	0.25	0.16	0.68	−0.05
Pulmonary involvement score	0.064	0.3	**0.004**	**0.3**	**0.041**	**0.21**	0.77	0.12	**0.002**	**0.33**	0.078	−0.18

Bold values indicate statistically significant result.

Funding

The study received no funding.

CRediT authorship contribution statement

All authors attest that they meet the current International Committee of Medical Journal Editors (ICMJE) criteria for Authorship.

Declaration of competing interest

The authors declare that they have no competing interest.

References

[1] Zhu N, Zhang D, Wang W, et al. A novel coronavirus from patients with pneumonia in China, 2019. N Engl J Med 2020 Feb 20;382(8):727–33 [PubMed PMID: 31978945. Pubmed Central PMCID: PMC7092803. Epub 2020/01/25. eng].
[2] Jin Y, Yang H, Ji W, et al. Virology, epidemiology, pathogenesis, and control of COVID-19. Viruses 2020 Mar 27;12(4) [PubMed PMID: 32230900. Pubmed Central PMCID: PMC7232198. Epub 2020/04/02. eng].
[3] Ng DL, Al Hosani F, Keating MK, et al. Clinicopathologic, immunohistochemical, and ultrastructural findings of a fatal case of Middle East respiratory syndrome coronavirus infection in the United Arab Emirates, April 2014. Am J Pathol 2016 Mar;186(3):652–8 [PubMed PMID: 26857507. Pubmed Central PMCID: PMC7093852. Epub 2016/02/10. eng].
[4] Faggiano P, Bonelli A, Paris S, et al. Acute pulmonary embolism in COVID-19 disease: preliminary report on seven patients. Int J Cardiol 2020 Aug 15;313:129–31 [PubMed PMID: 32471650. Pubmed Central PMCID: PMC7250100 construed as a conflict of interest. Epub 2020/05/31. eng].
[5] Bi X, Su Z, Yan H, et al. Prediction of severe illness due to COVID-19 based on an analysis of initial fibrinogen to albumin ratio and platelet count. Platelets 2020 May 5:1–6 [PubMed PMID: 32367765. Pubmed Central PMCID: PMC7212543. Epub 2020/05/06. eng].
[6] Wang D, Yin Y, Hu C, et al. Clinical course and outcome of 107 patients infected with the novel coronavirus, SARS-CoV-2, discharged from two hospitals in Wuhan, China. Crit Care 2020 Apr 30;24(1):188 [PubMed PMID: 32354360. Pubmed Central PMCID: PMC7192564. Epub 2020/05/02. eng].
[7] Favaloro EJ, Lippi G. Recommendations for minimal laboratory testing panels in patients with COVID-19: potential for prognostic monitoring. Semin Thromb Hemost 2020 Apr;46(3):379–82 [PubMed PMID: 32279286. Epub 2020/04/13. eng.].
[8] Tan C, Huang Y, Shi F, et al. C-reactive protein correlates with computed tomographic findings and predicts severe COVID-19 early. J Med Virol 2020 Jul;92(7):856–62 [PubMed PMID: 32281668. Pubmed Central PMCID: PMC7262341. Epub 2020/04/14. eng].
[9] Wu J, Wu X, Zeng W, et al. Chest CT findings in patients with coronavirus disease 2019 and its relationship with clinical features. Invest Radiol 2020;55(5):257–61. May. [PubMed PMID: 32091414. Pubmed Central PMCID: PMC7147284. Epub 2020/02/25. eng].
[10] Guan CS, Lv ZB, Yan S, et al. Imaging features of coronavirus disease 2019 (COVID-19): evaluation on thin-section CT. Acad Radiol 2020 May;27(5):609–13 [PubMed PMID: 32204990. Pubmed Central PMCID: PMC7156158. Epub 2020/03/25. eng].
[11] Chen A, Huang J, Liao Y, et al. Differences in clinical and imaging presentation of pediatric patients with COVID-19 in comparison with adults. Radiol Cardiothor Imag 2020;2(2):e200117.
[12] Chen Z, Fan H, Cai J, et al. High-resolution computed tomography manifestations of COVID-19 infections in patients of different ages. Eur J Radiol 2020 May;126:108972 [PubMed PMID: 32240913. Pubmed Central PMCID: PMC7102649. Epub 2020/04/03. eng].
[13] Fan N, Fan W, Li Z, Shi M, Liang Y. Imaging characteristics of initial chest computed tomography and clinical manifestations of patients with COVID-19 pneumonia. Jpn J Radiol 2020 Jun;38(6):533–8 [PubMed PMID: 32318916. Pubmed Central PMCID: PMC7171599. Epub 2020/04/23. eng].
[14] Bayramoglu Z, Canıpek E, Comert RG, et al. Imaging features of pediatric COVID-19 on chest radiography and chest CT: a retrospective, single-center study. Acad Radiol 2021 Jan;28(1):18–27 [PubMed PMID: 33067091. Pubmed Central PMCID: PMC7534757. Epub 2020/10/18. eng].
[15] Steinberger S, Lin B, Bernheim A, et al. CT features of coronavirus disease (COVID-19) in 30 pediatric patients. AJR Am J Roentgenol 2020 May;22:1–9 [PubMed PMID: 32442030. Epub 2020/05/23. eng].
[16] Li W, Cui H, Li K, Fang Y, Li S. Chest computed tomography in children with COVID-19 respiratory infection. Pediatr Radiol 2020 May;50(6):796–9 [PubMed PMID: 32162081. Pubmed Central PMCID: PMC7080075. Epub 2020/03/13. eng].
[17] Duan YN, Zhu YQ, Tang LL, Qin J. CT features of novel coronavirus pneumonia (COVID-19) in children. Eur Radiol 2020 Apr 14:1–7 [PubMed PMID: 32291501. Pubmed Central PMCID: PMC7156230. Epub 2020/04/16. eng].
[18] Liu M, Song Z, Xiao K. High-resolution computed tomography manifestations of 5 pediatric patients with 2019 novel coronavirus. J Comput Assist Tomogr 2020 May/Jun;44(3):311–3 [PubMed PMID: 32217900. Pubmed Central PMCID: PMC7228449. Epub 2020/03/29. eng].
[19] Lan L, Xu D, Xia C, Wang S, Yu M, Xu H. Early CT findings of coronavirus disease 2019 (COVID-19) in asymptomatic children: a single-center experience. Korean J Radiol 2020 Jul;21(7):919–24 [PubMed PMID: 32524792. Epub 2020/06/12. eng].
[20] Lu Y, Wen H, Rong D, Zhou Z, Liu H. Clinical characteristics and radiological features of children infected with the 2019 novel coronavirus. Clin Radiol 2020 Jul;75(7):520–5 [PubMed PMID: 32389373. Pubmed Central PMCID: PMC7252054. Epub 2020/05/12. eng].
[21] Hansell DM, Bankier AA, MacMahon H, McLoud TC, Müller NL, Fleischner Remy J. Society: glossary of terms for thoracic imaging. Radiology 2008 Mar;246(3):697–722 [PubMed PMID: 18195376. Epub 2008/01/16. eng].
[22] Zhu T, Wang Y, Zhou S, Zhang N, Xia L. A comparative study of chest computed tomography features in young and older adults with corona virus disease (COVID-19). J Thorac Imaging 2020 Mar 31;35(4):W97–101 [PubMed PMID: 32235187. Pubmed Central PMCID: PMC7253040. Epub 2020/04/03. eng].
[23] Wang J, Xu Z, Wang J, et al. CT characteristics of patients infected with 2019 novel coronavirus: association with clinical type. Clin Radiol 2020 Jun;75(6):408–14 [PubMed PMID: 32327229. Pubmed Central PMCID: PMC7138387. Epub 2020/04/25. eng].
[24] Yoon SH, Lee KH, Kim JY, et al. Chest radiographic and CT findings of the 2019 novel coronavirus disease (COVID-19): analysis of nine patients treated in Korea. Korean J Radiol 2020 Apr;21(4):494–500 [PubMed PMID: 32100485. Pubmed Central PMCID: PMC7082662. Epub 2020/02/27. eng].
[25] Xiong Y, Sun D, Liu Y, et al. Clinical and high-resolution CT features of the COVID-19 infection: comparison of the initial and follow-up changes. Invest Radiol 2020 Jun;55(6):332–9 [PubMed PMID: 32134800. Pubmed Central PMCID: PMC7147282. Epub 2020/03/07. eng].
[26] Pan F, Yang L, Li Y, et al. Factors associated with death outcome in patients with severe coronavirus disease-19 (COVID-19): a case-control study. Int J Med Sci 2020;17(9):1281–92 [PubMed PMID: 32547323. Pubmed Central PMCID: PMC7294915. Epub 2020/06/18. eng].
[27] Li K, Wu J, Wu F, et al. The clinical and chest CT features associated with severe and critical COVID-19 pneumonia. Invest Radiol 2020 Jun;55(6):327–31 [PubMed PMID: 32118615. Pubmed Central PMCID: PMC7147273. Epub 2020/03/03. eng].
[28] Zhang ZL, Hou YL, Li DT, Li FZ. Laboratory findings of COVID-19: a systematic review and meta-analysis. Scand J Clin Lab Invest 2020 May 23:1–7 [PubMed PMID: 32449374. Pubmed Central PMCID: PMC7256350. Epub 2020/05/26. eng].